https://doi.org/10.3311/PPch.41048

Periodica Polytechnica Chemical Engineering, 69(4), pp. 673–684, 2025

Development and Physicochemical Analysis of SrO/Hydroxyapatite Modified Mineral Trioxide Aggregate Synthesized from Calcium Carbonate and Tetraetyl Ortosilicate as an Endodontic Material

Leny Yuliatun[1*], Mariyam Mariyam[2**], Mahardika Fahrudin Rois[3], Lia Destiarti[4], Dita Ariyanti[5], Erlin Purwita Sari[6], Hidayatul Fajri MS[7], Nuzul Ficky Nuswantoro[1], Hadiyawarman Hadiyawarman[3]

[1] Research Center for Biomass and Bioproducts, National Research and Innovation Agency, Raya Puspitek 60, 15314 South Tangerang, Indonesia
[2] Department of Chemistry, Faculty of Science, Institut Teknologi Sumatera, Jl. Terusan Ryacudu, Jati Agung, 35365 Lampung, Indonesia
[3] Research Center for Advanced Materials, National Research and Innovation Agency, Raya Puspitek 60, 15314 South Tangerang, Indonesia
[4] Department of Chemistry, Faculty of Mathematics and Natural Sciences, Universitas Tanjungpura, Jenderal Ahmad Yani, 78114 Pontianak, Indonesia
[5] Research Center for Applied Microbiology, National Research and Innovation Agency, Jl. Raya Jakarta-Bogor km 46, 16911 Cibinong, Indonesia
[6] Directorate of Laboratory Management, Research Facilities, and Science, and Technology Park, National Research and Innovation Agency, Gunungkidul, 55281 Yogyakarta, Indonesia
[7] Biomedic Research Center, National Research and Innovation Agency, Jl. Raya Jakarta-Bogor km 46, 16911 Cibinong, Indonesia
* Corresponding author, e-mail: leny004@brin.go.id
** Second corresponding author, e-mail: mariyam@ki.itera.ac.id

Received: 17 May 2025, Accepted: 22 October 2025, Published online: 24 November 2025

Abstract

Mineral trioxide aggregate (MTA) is utilized in endodontics for root fracture repair, apexification, and as a root canal filling material. MTA possesses favorable sealing capability and biocompatibility. However, its clinical performance is limited by low mechanical performance at the early stage of hydration. In the present study, the limitations of MTA were addressed by incorporating SrO and hydroxyapatite (HA) into its formulation. MTA was synthesized using calcium carbonate as the calcium oxide precursor and tetraethyl orthosilicate as the silica source. The synthesis employed a sol–gel method followed by a solid-state calcination process at 1000 °C. The hydration of material was performed with water at a powder-to-liquid ratio of 3:1 (w/v). The study found that incorporation of 5% SrO into MTA enhanced the formation of calcium silicate hydrate (C–S–H) phases, as evidenced by increased X-ray diffraction peak intensity at 2θ = 29.3°. This modification also increased the compressive strength after seven days of hydration, sustaining an alkaline pH environment. MTA composite containing 5% SrO combined with 6% HA further amplified the intensity of C–S–H formation. Morphological analysis showed that the development of hydration reaction reduced porosity and voids, yielding a more regular microstructure. An increase in HA concentration leads to a decrease in the pH of the material, trending toward neutrality by days 7 and 28. Such pH modulation can reduce the localized acidity and thereby minimize inflammatory responses when the material is applied in biological settings.

Keywords

mineral trioxide aggregate, SrO, hydroxyapatite, physicochemical

1 Introduction

Materials used in endodontic therapy following root canal treatment continue to undergo significant development. Mineral trioxide aggregate (MTA) has attracted attention due to its bioactive properties, particularly its ability to form apatite upon contact with biological fluids. When MTA comes into contact with a liquid medium, the released Ca^{2+} ion reacts with phosphate ions in saliva to form apatite crystal deposits [1]. This process facilitates remineralization at

Cite this article as: Yuliatun, L., Mariyam, M., Rois, M. F., Destiarti, L., Ariyanti, D., Purwita Sari, E., Fajri MS, H., Ficky Nuswantoro, N., Hadiyawarman, H. "Development and Physicochemical Analysis of SrO/Hydroxyapatite Modified Mineral Trioxide Aggregate Synthesized from Calcium Carbonate and Tetraetyl Ortosilicate as an Endodontic Material", Periodica Polytechnica Chemical Engineering, 69(4), pp. 673–684, 2025. https://doi.org/10.3311/PPch.41048

the dentin-MTA interface. The resulting apatite layer provides a strong interaction between dentin and pulp tissue, thereby promoting the repair and regeneration of the tooth's mineralized hard tissues. In many studies, commercially available MTA, such as ProRoot MTA, is employed as a standard reference material [1]. Its composition comprises 80% calcium silicate (derived from Portland cement) and 18–20% radiopacifying agents [2].

Radiopacity agents in endodontic materials generally consist of metal oxides from elements with high atomic numbers. These oxides often originate from transition metals such as zirconium, titanium, and zinc. However, excessive incorporation of these oxides may induce cytotoxic effects, that affect the biocompatibility of MTA. A radiopacifier such as bismuth oxide (Bi_2O_3) has notable limitations because it is hydrophobic in nature which leads to bubble formation during MTA hydration and increases the brittleness of the material [3]. This formulation is closely linked to reduced compressive strength and increased solubility. This behavior arises from weak interparticle bonding within the aggregate matrix, facilitating dissolution in aqueous environments such as saliva [1]. As a result, the long-term mechanical stability and load-bearing capacity of MTA are affected.

To overcome these limitations, incorporating oxide compounds has been explored to reinforce the aggregate structure, thereby improving compressive strength, dimensional stability, and resistance to dissolution. Enhancing the MTA stability strengthens its physical properties and improves adhesion to dental hard tissues, ultimately contributing to greater biomechanical compatibility and clinical efficacy in hard tissue regeneration.

One approach to improving the compressive strength and radiopacity of MTA to meet ISO 6876:2001 [4] and ANSI/ADA 57-2021 [5] standards (radiopacity >3 mm Al) is the incorporation of SrO. The incorporation of SrO into MTA enables the substitution of Ca^{2+} ions, thereby enhancing structural stability by reinforcing the calcium silicate lattice within the material without losing its radiopacity properties [6, 7]. In addition, the incorporation of hydroxyapatite (HA) has been shown to further improve both the bioactivity and adhesive properties of MTA [8, 9]. Following hydration, HA contributes to mechanical reinforcement by filling microgaps and voids within the matrix, forming a denser and more rigid structure [10]. The effect of HA on compressive strength is concentration-dependent. At low to moderate pH levels, HA acts as a reinforcing filler that reduces porosity and increases overall density, leading to improved mechanical integrity. However, when the HA content exceeds the optimal composition, detrimental effects occur; the material becomes more brittle and susceptible to cracking due to particle agglomeration and the relatively lower intrinsic strength of HA. This behavior differs from other inert bioceramics such as alumina and zirconia, which typically exhibit a linear increase in compressive strength with higher filler loading due to their stable mechanical properties and lack of bioactive interactions [1, 11].

Previous studies have investigated the incorporation of SrO and HA into MTA, demonstrating enhancements in compressive strength and dentin-MTA interface bonding [1]. However, most of these studies were limited to short-term hydration periods (≤ 14 days), providing insufficient insight into the long-term stability and maturation of calcium silicate hydrate (C–S–H) phases, which are critical for mechanical performance and biological activity. Prior research often excluded artificial saliva immersion for solubility, pH, and calcium ions release assessment, an essential factor for simulating the oral environment for endodontic application. Moreover, MTA synthesis has predominantly relied on physical solid-state techniques such as ball milling, rather than advanced wet-chemical synthesis approaches like sol–gel processing [12].

The present study addresses these limitations by systematically evaluating the *in vitro* physicochemical and mechanical properties of MTA modified with SrO and HA across different hydration durations. Furthermore, the influence of hydration and subsequent artificial saliva immersion on compressive strength, calcium ion release, and alkalinity were assessed. By integrating extended hydration times with a simulated oral environment and advanced synthesis methodologies, this study provides a more comprehensive evaluation of MTA performance and its potential clinical applicability.

The present study addresses these gaps by systematically evaluating the *in vitro* physicochemical properties of MTA modified with SrO and HA with varying hydration time. MTA was synthesized using CaO, SiO_2 and Al_2O_3. The present study aims to systematically evaluate the *in vitro* physicochemical properties of synthesized materials over varying hydration durations. In addition, the effects of hydration and subsequent immersion in artificial saliva on compressive strength, calcium ion release, and alkalinity were assessed. This approach provides a more comprehensive understanding of MTA performance under clinically relevant conditions and explores how advanced synthesis methodologies influence material behavior.

2 Materials and methods

2.1 Materials

The raw materials used for synthesis were purchased from Sigma-Aldrich (Germany). Bismuth trioxide (Bi_2O_3), aluminum nitrate nonahydrate ($Al(NO_3)_3 \cdot 9H_2O$, ≥99% purity), calcium carbonate ($CaCO_3$, ≥99% purity), and tetraethoxyorthosilicate (TEOS, ≥99% purity) were utilized with 25% ammonia solution catalyzing the sol–gel MTA synthesis. For MTA modification, $SrCO_3$ (≥98% purity) and HA (≥99% purity) were incorporated.

2.2 Characterization methods

Phase identification and crystallinity were determined using X-ray diffraction (XRD, X'Pert Pro diffractometer) with scans collected over a 2θ range of 5°–80° using Cu-Kα radiation (40 kV, 30 mA). Functional groups and bonding characteristics were analyzed by Fourier transform infrared (FTIR) spectroscopy (Shimadzu 8201PC). Morphological features were examined by scanning electron microscopy (SEM, JEOL), and elemental composition was quantified using an atomic absorption spectrophotometer (AAS, Analytic Jena). The pH values during hydration were measured with a Mettler Toledo pH meter, and the compressive strength was evaluated using a universal testing machine (Texture Analyzer CT3 Brookfield) at a crosshead speed of 10 mm min^{-1}.

2.3 Synthesis method

MTA materials were synthesized using a combined sol–gel and solid-state reaction method [1, 13]. Following the process, HA was incorporated as a secondary modifier. Initially, 200 mL of deionized water was mixed with 1% v/v concentrated ammonia solution (25%) as a base catalyst and stirred. TEOS (20 wt%) and $CaCO_3$ (60 wt%) were added, followed by continuous stirring. Subsequently, 2 wt% $Al(NO_3)_3 \cdot 9H_2O$ was introduced as Al_2O_3 source, and $SrCO_3$ was added at varying concentrations of 5, 7.5, and 10 wt% (corresponding to the equivalent SrO content after calcination). The mixture was stirred and heated at 80 °C until a solid gel formed. The resulting white gel was dried and calcined at 1000 °C for 3 h, then blended with Bi_2O_3 at concentrations of 13, 10.5, and 8 wt% (with all oxide components totaling 100 wt%). The calcined product was sieved through a 200-mesh (74 μm) sieve, yielding a yellowish-white powder designated as MTA modified with SrO (MTAS). For further modification, MTAS containing 5 wt% SrO was supplemented with HA at 3, 6, and 9 wt% concentrations. The powders were homogenized, sieved (200 mesh, 74 μm), and designated as MTASH. The composition of all synthesized materials was presented in Table 1. The synthesized materials (MTAS and MTASH) were characterized alongside a commercial MTA (ProRoot) used as the control for comparison.

2.4 Compressive strength test

Hydrated MTA and modified MTA samples were prepared by mixing the powder with deionized water at a powder-to-liquid ratio of 3:1. The mixtures were then placed into cylindrical molds (4 mm diameter × 6 mm height) to form test specimens in accordance with ISO 9917-1:2025 guidelines [14]. Compressive strength was evaluated on samples cured for 1, 3, and 7 days. The results were recorded based on the maximum load at failure and reported in MPa.

2.5 pH, solubility and calcium ion release assessment

Specimens of the hydrated materials (4 mm diameter × 3 mm height) were immersed in 2.5 mL of artificial saliva and allowed to set for 24 h. The solubility was determined by measuring specimen mass before and after 24 h of immersion in accordance with ISO 6876:2001 [4] guidelines.

The alkalinity and calcium ion release of the immersion medium were measured at 1, 7, and 28 days using a calibrated pH meter and atomic absorption spectroscopy, respectively. The alkalinity and calcium ion release tests follow adapted protocols consistent with ISO 6876:2001 [4] solubility.

3 Result and discussion

3.1 Compressive strength test

The compressive strength testing was conducted to evaluate the mechanical stability of the synthesized materials. In the compressive strength test, the material is positioned vertically on the instrument according to ISO 9917-1:2025 standard [14]. As illustrated in Fig. 1, the compressive strength of the materials increased gradually with hydration time. This improvement is primarily attributed to

Table 1 Composition of synthesized materials (wt%)

Groups*	SrO (%)	HA (%)	Bi_2O_3 (%)
MTAS0	0	0	18
MTAS5	5	0	13
MTAS7.5	7.5	0	10.5
MTAS10	10	0	8
MTAS5H3	5	3	13
MTAS5H6	5	6	13
MTAS5H9	5	9	13

* MTA refers to the laboratory-synthesized compound

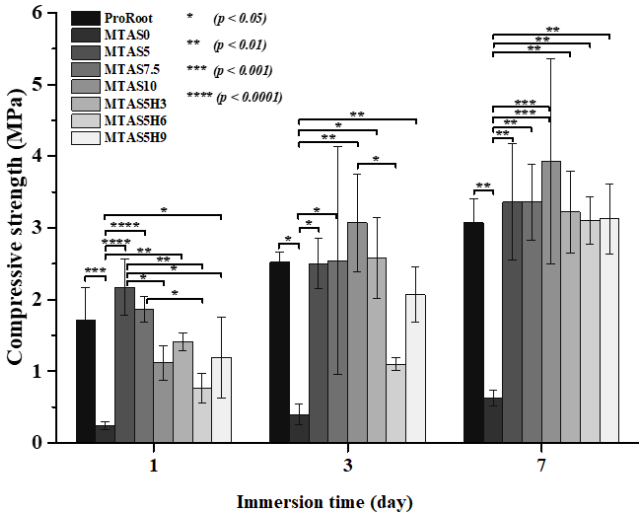

Fig. 1 Compressive strength test of materials variations at different curing periods (1, 3, and 7 days)

the formation of C–S–H gel, which continues to develop and typically reaches full maturity by approximately 28 days [15]. Within this process, tricalcium silicate (C_3S) serves as a key phase, releasing calcium ions and silica that react to form stable C–S–H bonds during hydration [16]. These reactions contribute to the development of a denser microstructure, thereby enhancing the mechanical integrity and long-term stability of the material.

According to Fig. 1, the compressive strength on the first day remained relatively low, which can be attributed to the early-stage hydration reactions and the incomplete setting of the cement matrix. Reported data indicate that the compressive strength of commercial MTA ranges between 2.87 and 3.63 MPa after one day of hydration [17, 18]. This value progressively increases, reaching approximately 67.3 MPa after 21 days, beyond which no significant improvement is observed, suggesting that the cement has achieved its mechanical stability [19]. The addition of SrO and HA significantly enhanced the compressive strength of the modified MTA compared to the unmodified one. Among the tested groups, MTA containing 5% SrO exhibited the highest compressive strength, reaching 2.17 MPa on day 1. This result is consistent with previous reports, where synthesized MTA demonstrated a compressive strength of approximately 2.09 MPa after one hydration day [13]. By days 3 and 7, the compressive strength showed a marked increase, particularly in samples with higher SrO content. This improvement can be attributed to the progressive development of crystallinity and the formation of stronger interparticle bonds. By the seventh day, most cementation and hydration reactions had stabilized, yielding a more stable microstructure and improved mechanical integrity [20].

The addition of HA tends to reduce the compressive strength of composite materials, primarily due to its low fracture toughness. Thus, incorporating HA to MTA requires an optimum composition to achieve a synergistic balance between mechanical reinforcement and sustained bioactivity [21, 22].

Bi_2O_3 is commonly used as a radiopacity agent in MTA to ensure radiographic visibility; however, it is chemically inert during the hydration process and does not disrupt the structure of MTA [23]. The addition of reinforcing oxides such as SrO has been explored, as SrO enhances the mechanical properties and maintains the radiopacity required for clinical applications [24]. Achieving an optimal balance between radiopacity, bioactivity, and mechanical properties remains an essential consideration in developing of advanced MTA formulations.

3.2 pH determination

The main mechanism of MTA in biological environments is the establishment of an alkaline pH that provides antibacterial conditions and promotes tissue repair by stimulating new tissue formation [25]. The results of pH measurements obtained using a calibrated pH meter are presented in Fig. 2. As shown in Fig. 2, all tested groups exhibited higher alkalinity than the ProRoot control with pH values ranging from 7.7 to 9.4. The pH increased with hydration time along with the gradual release of hydroxyl ions from calcium hydroxide generated during the reaction of calcium ions with water. Such an alkaline environment favors cementitious reactions and support tissue healing, consistent with previous reports [25, 26].

The pH increase observed at day 7 suggests the continuation of the hydration reactions. By day 28, the pH values

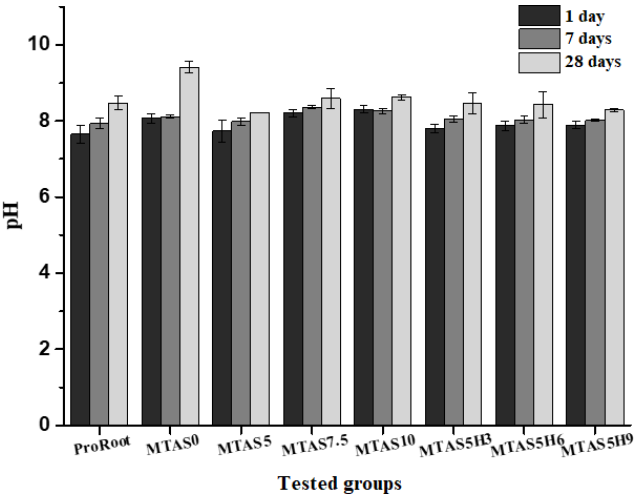

Fig. 2 pH test of materials variations at different curing periods (1, 7, and 28 days)

approached a plateau, indicating that the cement matrix had largely stabilized, in agreement with the findings of Zhang et al. [25]. Commercial MTA usually exhibits an alkaline pH, typically around 12.5 after setting due to calcium hydroxide formation [27]. Notably, fluctuations in pH observed on certain days can be linked to the release of strontium ions, which may increase the pH of the immersion solution. The Ca^{2+} and Sr^{2+} ion release and potentially influence subsequent cellular responses [28].

Ca^{2+} ion released from the dissociation of calcium hydroxide may react with phosphate ions present in saliva to form apatite crystals, a mineral phase essential for tissue repair and regeneration. This reaction is accompanied by the continued release of OH^-, which maintain an alkaline environment. The presence of Ca^{2+} and OH^- is a defining characteristic of the bioactivity of MTA, as it preserves a high pH over extended periods. This prolonged alkalinity is widely recognized as a critical factor in stimulating hard tissue formation and facilitating biological healing processes [29].

An alkaline pH, typically in the range of 8–9, is beneficial in reducing the risk of irritation to soft tissues such as the gingiva. Within the context of dental materials, this degree of alkalinity not only facilitates hard tissue mineralization but also contributes to antimicrobial efficacy [30]. Ideally, restorative materials intended for hard tissue repair should sustain an alkaline environment, as lower pH conditions can lead to erosion of dental structures. Therefore, maintaining an optimum alkaline pH is critical both for the protection of dental tissues and the promotion of effective healing.

3.3 Solubility

Solubility refers to the extent of dissolution of MTA when exposed to aqueous media. Such dissolution may significantly influence the mechanical strength, dimensional stability, and overall clinical performance of MTA. During hydration, reactions between MTA and the surrounding fluid medium may lead to partial material degradation, resulting in measurable mass loss. Evaluation of this parameter, particularly within the first 24 h, is critical as it provides insight into the initial stability and clinical suitability of the material [31, 32]. Materials exhibiting minimal mass loss are generally more stable and thus more reliable for endodontic applications compared to those with higher dissolution rates. The results of the mass loss evaluation are presented in Fig. 3.

The solubility test was conducted in accordance with ISO 6876:2012 standard [33] (less than 3% solubility) and evaluated after one day of immersion. As shown in Fig. 3,

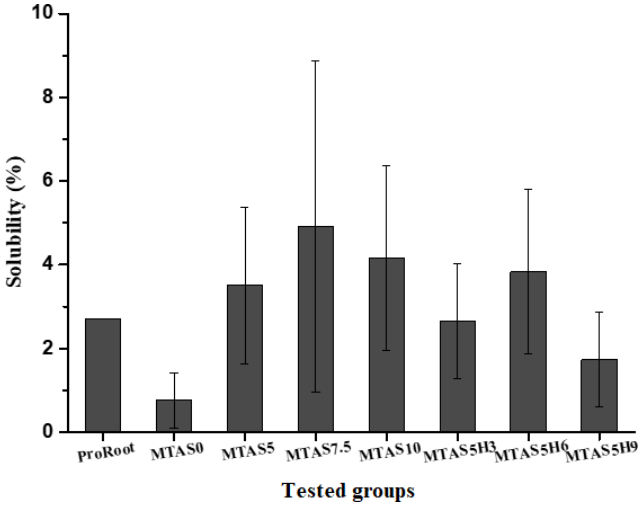

Fig. 3 Solubility test of materials after 1 day immersion in artificial saliva

the mass loss observed at the early stage indicated the ongoing hydration and setting reactions of the cement matrix. The synthesized MTA samples (MTAS0, MTAS5H3, and MTAS5H9) complied with the ISO 6876:2001 standard [4], exhibiting mass losses below 3%. In contrast, formulations such as MTAS5, MTAS7.5, MTAS10, and MTAS5H6 demonstrated mass losses exceeding 3%.

Among the tested samples, MTAS7.5 exhibited the highest mass loss (4.91%), indicating low structure stability, weaker interfacial bonding, and incomplete cement formation. This instability may be associated with the incorporation of SrO, which promotes the formation of strontium silicate phases. As a consequence, fewer calcium ions participate in the formation of C–S–H. At the same time, a larger fraction of Ca^{2+} remains unbound and is released into the surrounding medium [1]. In contrast, the MTAS0 sample demonstrated the lowest solubility, likely due to the absence of competing strontium silicate formation, which allows silica to fully interact with calcium and yield a more stable calcium silicate matrix.

The incorporation of HA can minimize solubility (mass loss) in MTA by maintaining an optimal balance during cement formation, as evidenced by the improved stability of MTAS5H3 and MTAS5H9. The low mass loss reflects the stability of MTA, indicating resistance to dissolution when exposed to surrounding biological fluids. This property is essential, as MTA typically exhibits lower solubility than other endodontic materials, a feature that contributes to its clinical performance in root canal therapy [32]. A tightly bonded cement matrix ensures structural integrity with low material degradation, essential for establishing a durable seal. Consequently, low solubility is considered a key criterion of advanced endodontic materials, as it enhances the sealing ability, minimizes microbial

penetration, reduces the potential of reinfection, and contributes to long-term clinical success.

3.4 Calcium ion release

The calcium ion release test quantifies the amount of Ca^{2+} ions dissolved into the surrounding liquid medium. It is a critical parameter for stimulating new tissue formation and supporting effective setting in moist environments. The calcium ion release profiles of the MTA samples are presented in Fig. 4. The Ca^{2+} release is related to the bioactivity of MTA, as Ca^{2+} ions contribute to the nucleation of apatite, stimulate cellular responses required for tissue regeneration, and participate in hydration reactions [25].

As shown in Fig. 4, most samples exhibited a gradual decline in calcium ion concentration with increasing hydration time. This reduction indicates progressive stabilization of the cement matrix as hydration reactions mature. Interestingly, the commercial control material (ProRoot MTA) displayed increased calcium ion release on day 28, suggesting that hydration reactions were still ongoing and that material had not yet reached the complete setting. In general, a decreasing or plateauing trend in calcium ion release over time reflects the establishment of a stable cement matrix, where ion release is limited by microstructural densification. Such behavior highlights the dynamic nature of cement hydration and provides a meaningful indicator of long-term stability, durability, and clinical performance.

Based on the calcium ion release profiles shown in Fig. 4, the relatively high release of Ca^{2+} on the first day contributes to elevating the pH of the surrounding medium, thereby creating an alkaline environment that inhibits bacterial growth. By day 7, calcium ion release decreases,

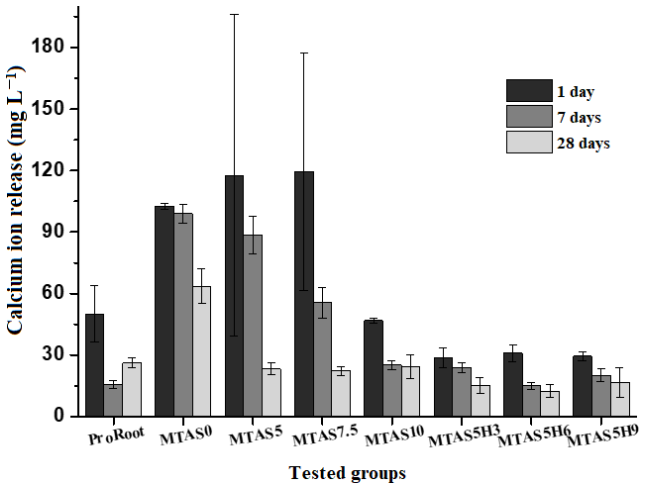

Fig. 4 Calcium ion release test of materials variations at different curing periods (1, 7, and 28 days)

although sufficient Ca^{2+} remains available to exert therapeutic effects. This reduction is associated with the progressive incorporation of calcium ions into hydration products, forming a more stable cement structure. By day 28, the crystallization of cement phases further densifies the hydration product (C–S–H), leading to reduced calcium ion release into the immersion medium. Moreover, the sustained and controlled release of Ca^{2+} maintains an alkaline environment that facilitates hard tissue regeneration and accelerates healing of the repaired tooth structure [34].

Incorporation of SrO into MTA has been shown to increase calcium ion release at early stages, thereby enhancing initial bioactivity. In contrast, the addition of HA tends to reduce calcium ion release, as the rapid formation of an apatite layer on the material surface facilitates hydration reactions and promotes earlier matrix stabilization [1].

Hard tissue formation induced by MTA is strongly associated with its capacity to release Ca^{2+}. These ions interact with PO_4^{3-} and OH^- species present in saliva, resulting in the precipitation of apatite-like phases on the MTA surface. This biomineralization process is critical for the mineralization of hard tissues and underpins the development of dentin bridges during root canal therapy. Sustained Ca^{2+} release facilitates mineral deposition and enhances the biological response by stimulating dental pulp tissue, thereby promoting healing and regeneration [35]. A stable release of calcium ions typically corresponds with consistent hydroxyl ion release, which maintains an alkaline environment over time. This prolonged alkalinity is essential to the bioactivity of MTA and contributes significantly to its favorable biological performance. Among the tested formulations, MTAS5H6 exhibited the most consistent calcium ion release after 28 days, suggesting greater potential to support hard tissue formation and accelerate tissue healing in clinical applications.

3.5 Crystallinity characteristics of hydration materials using XRD

XRD analysis was performed after hydration to investigate the interaction of water with MTA. This technique enables the identification of crystalline phase evolution during hydration and setting. The diffractograms presented in Fig. 5 illustrate the phases formed at this early stage, providing critical information on the structural transformations occurring within the material. Such changes are directly correlated with the mechanical performance and bioactivity of MTA in dental applications.

After 7 days of hydration in distilled water, the XRD patterns shown in Fig. 5 display a distinct $Ca(OH)_2$ peak at

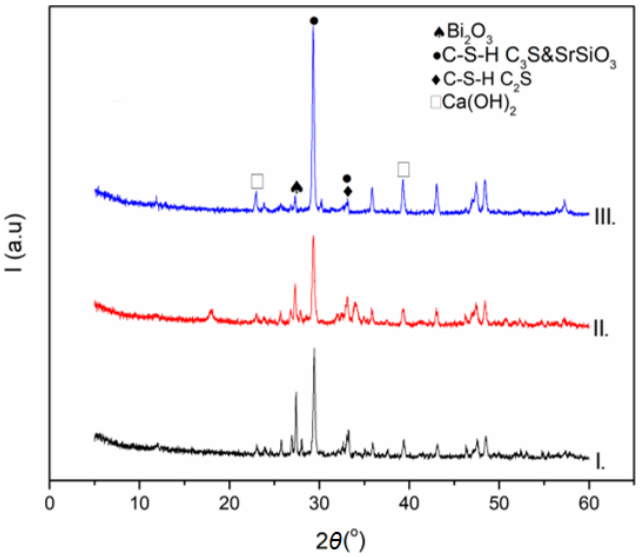

Fig. 5 Diffractograms of hydrated materials: I. MTAS0; II. MTAS5; III. MTAS5H6

$2\theta \approx 25.8°$, consistently observed across both commercial and experimental samples. Notably, the intensity of the tricalcium silicate (Ca_3SiO_5) peak at $2\theta \approx 29.3°$ increased with the incorporation of SrO (Fig. 5 diffractograms II. and III.). This observation suggests an active hydration reaction in which Ca_3SiO_5 progressively converts into C–S–H as the primary product responsible for the setting and mechanical reinforcement of the cement matrix [36]. The formation of C–S–H gel not only strengthens the microstructure but also enhances the bioactivity of the material. These hydration-driven transformations are fundamental to the development of the structural integrity and biological functionality of MTA during its early interactions with liquid environments in the oral cavity.

Tricalcium silicate plays a crucial role in governing hydration reactions and the development of compressive strength in MTA. The diffraction peaks of tricalcium silicate and strontium silicate often overlap, complicating their distinction. Importantly, the strontium silicate peak shifts to lower diffraction angles from its original position at around $2\theta = 33.5°$. As the hydration reaction progresses, the appearance of a new peak at $2\theta = 34.3°$ indicates the progressive conversion of tricalcium silicate into C–S–H [37]. Furthermore, the diffraction peaks at $2\theta = 34.3°$ and 47.1° are characteristic of calcium hydroxide (portlandite, ICDD 44-1481). These crystallographic changes indicate the structural transformations occurring during hydration, which are directly correlated with the strengthening and stabilization of the cement matrix.

The main hydration product of MTA is C–S–H, which determines the mechanical strength, structural stability, and resistance to compressive forces [13]. Concurrently, $Ca(OH)_2$ is generated as a by-product of the reaction between calcium silicate phases and water. This compound contributes to the antibacterial activity of MTA and elevates the environmental pH, thereby creating favorable conditions for tissue healing [23]. Ca_3SiO_5, one of the initial crystalline phases, progressively diminishes during hydration as it is consumed in the formation of C–S–H product. The gradual reduction of unhydrated tricalcium silicate, accompanied by the increasing presence of C–S–H, reflects the progression of the setting reaction and the maturation of the cement matrix.

3.6 Functional group of materials after hydration using FTIR

FTIR spectroscopy was employed to characterize the functional groups present after hydration of the MTA. The resulting spectra, presented in Fig. 6, reveal the chemical transformations and molecular interactions associated with the early stages of cement setting. The FTIR spectra in Fig. 6 display several characteristic absorption bands corresponding to hydration products and the molecular structure of the MTA materials. A broad band at ~3450 cm^{-1} is assigned to O–H stretching vibrations of calcium hydroxide generated during hydration, while the peak near 1650 cm^{-1} corresponds to the H–O–H bending mode of molecular water within the hydrated matrix. An absorption band at ~1400 cm^{-1} indicates carbonate groups, likely originating from atmospheric carbonation of $Ca(OH)_2$ or residual unreacted calcium carbonate. In the region of 935–995 cm^{-1}, Si–O stretching vibrations are observed, characteristic of silicate groups in the cement structure.

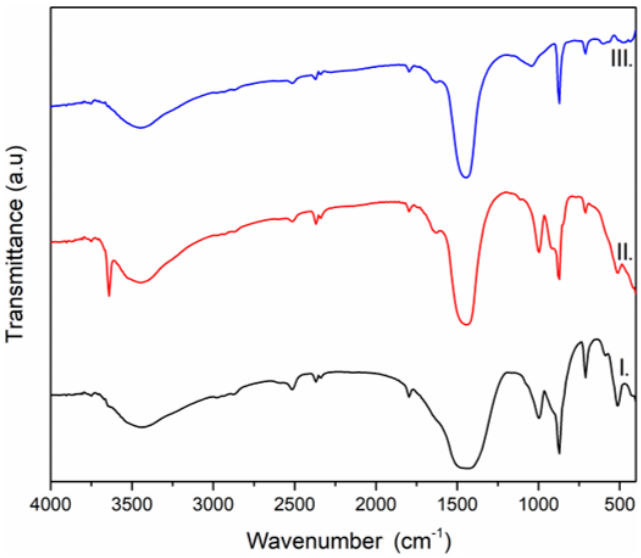

Fig. 6 Infrared spectra of hydrated materials: I. MTAS0; II. MTAS5; III. MTAS5H6

The 1000–1100 cm^{-1} region is dominated by Si–O stretching vibrations associated with C–S–H gel, the primary hydration phase that imparts mechanical strength and structural stability. Additional bands between 570 and 600 cm^{-1} correspond to Si–O–Si bending vibrations, indicative of C–S–H formation. The band near 525 cm^{-1} is attributed to hydration reactions involving alite and belite phases, confirming the presence of ongoing cementitious processes during setting [22].

In Fig. 6 (infrared spectra I.–III.), the broadening of the O–H stretching band at ~3448 cm^{-1} after hydration reflects the incorporation of water within the cement matrix [38]. The spectrum of the unmodified MTA sample (Fig. 6, infrared spectrum I.) exhibits a broader and more intense O–H absorption band, consistent with the material's hygroscopic nature. Incorporation of 5 wt% SrO, either alone or in combination with 6 wt% HA, reduces this band intensity, suggesting decreased water uptake. This behavior is consistent with the hydrophilic characteristics of MTA at room temperature, governed by the presence of Ca_3SiO_5 [39]. The Ca–O vibration band at ~1473 cm^{-1} also shows reduced intensity after SrO or SrO–HA incorporation, likely due to the diminished hygroscopicity and reduced water binding capacity of the modified materials.

After 7 days of hydration (Fig. 6, infrared spectrum II.), a sharp O–H stretching band characteristic of portlandite [$Ca(OH)_2$] emerges at 3641 cm^{-1}, accompanied by a smaller band between 740–750 cm^{-1} corresponding to C–S–H [40]. SrO addition influences the hydration reaction by limiting calcium's interaction with silica to form C–S–H, favoring $Ca(OH)_2$ formation and the release of hydroxyl ions. The persistent O–H vibration band attributed to portlandite in the MTAS5 can be explained by the relatively higher hydration tendency of SrO compared with CaO, resulting in the formation of $Sr(OH)_2$, further contributing to the portlandite absorption intensity.

3.7 Surface morphology of material before and after hydration

Scanning electron microscopy was employed to examine the microstructure and surface morphology of the MTA materials. Representative SEM images obtained before and after hydration are shown in Fig. 7. As illustrated in Fig. 7 (a), the unhydrated MTA exhibits irregularly shaped, agglomerated particles with rough surface textures and relatively large porous regions. Following the incorporation of SrO and HA (MTAS5H6), the particle morphology becomes more refined and homogeneous, yielding a denser

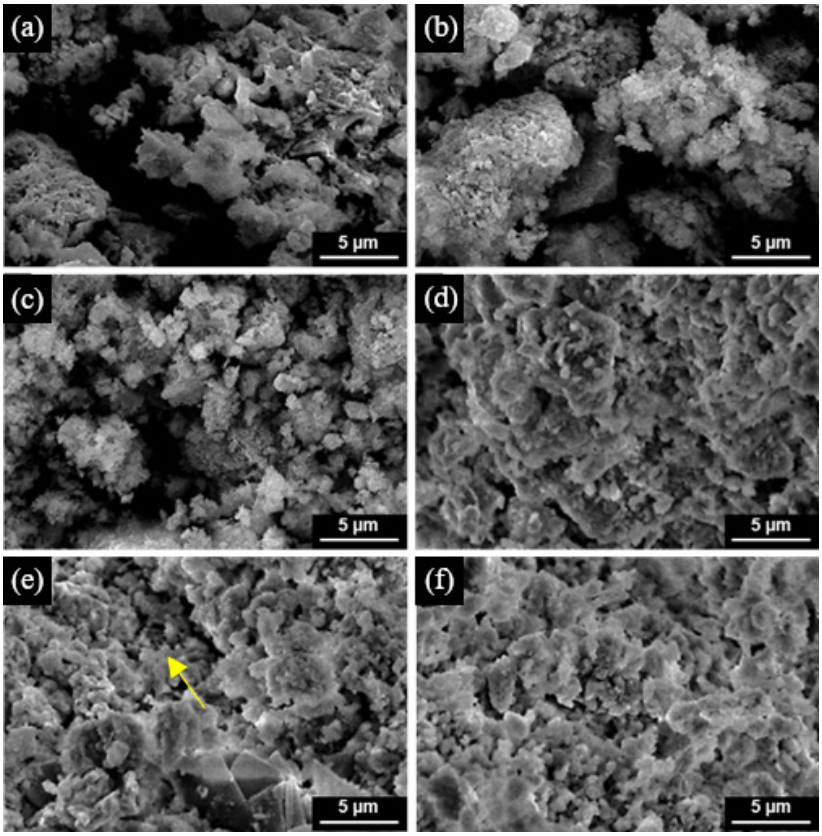

Fig. 7 SEM images of uh-hydrated materials: (a) MTAS0; (b) MTAS5; (c) MTAS5H6 and after 7 days of hydration; (d) MTAS0; (e) MTAS5; (f) MTAS5H6 (with 5000× magnification)

and more compact microstructure upon hydration. This tighter packing reduces pores and voids, improving sealing ability and enhancing mechanical stability when applied to dental tissues. The images also reveal particle aggregation in clusters and plate-like shapes, along with residual porosity characteristic of the hydrated matrix [41, 42]. Such microstructural modifications are directly linked to the mechanical performance and bioactivity of the material.

Based on the micrographs in Fig. 7, hydration of the MTA material led to the formation of C–S–H aggregates, accompanied by a reduction in voids and overall porosity (Fig. 7 (d)). Surface roughness was also reduced compared to the pre-hydration state. During this process, the initially dispersed particles consolidated into a denser and more cohesive microstructure, thereby minimizing interparticle gaps. These microstructural changes indicate effective material hardening, consistent with proper cementation and enhanced structural strength.

The hydrated MTA sample containing 5 wt% SrO exhibited larger and denser particle agglomerates relative to the SrO-free formulation (Fig. 7 (e)). Distinct crystalline calcium hydroxide structures were observed, appearing as needle-like, prismatic, and triangular morphologies, typical of hydration products. In addition, the incorporation of SrO promoted the formation of apatite crystals interconnecting these agglomerates, as highlighted by arrows in Fig. 7 (e). These fibers are commonly generated in phosphate-rich environments through Ca^{2+} release and are capable of penetrating dentinal tubules, thereby enhancing the material's bioactivity [43]. The sample modified with 5 wt% SrO and 6 wt% HA displayed smaller, more compact, and uniformly shaped particle clusters compared with both unmodified MTA and the SrO-only formulation (Fig. 7 (f)). This refined microstructure suggests improved cohesion and potentially superior long-term stability.

Overall, the surface morphology results shown in Fig. 7 demonstrate that incorporation of SrO and HA reduces the formation of gaps, cavities, and pores within the cement matrix. This improvement promotes the development of apatite fibers during hydration, enhancing compressive strength and facilitating more interaction to dentin. The capacity of these modified materials to maintain such properties under biologically relevant conditions can be further validated through immersion in artificial saliva, simulating in vivo performance on dental hard tissues.

3.8 Mapping of hydrated and un-hydrated materials

SEM elemental mapping was conducted before and after 7 days of hydration in distilled water to evaluate elemental distribution and compositional changes following fluid interaction. The mapping results in Fig. 8 visualize the elemental distribution of hydrated and un-hydrated materials.

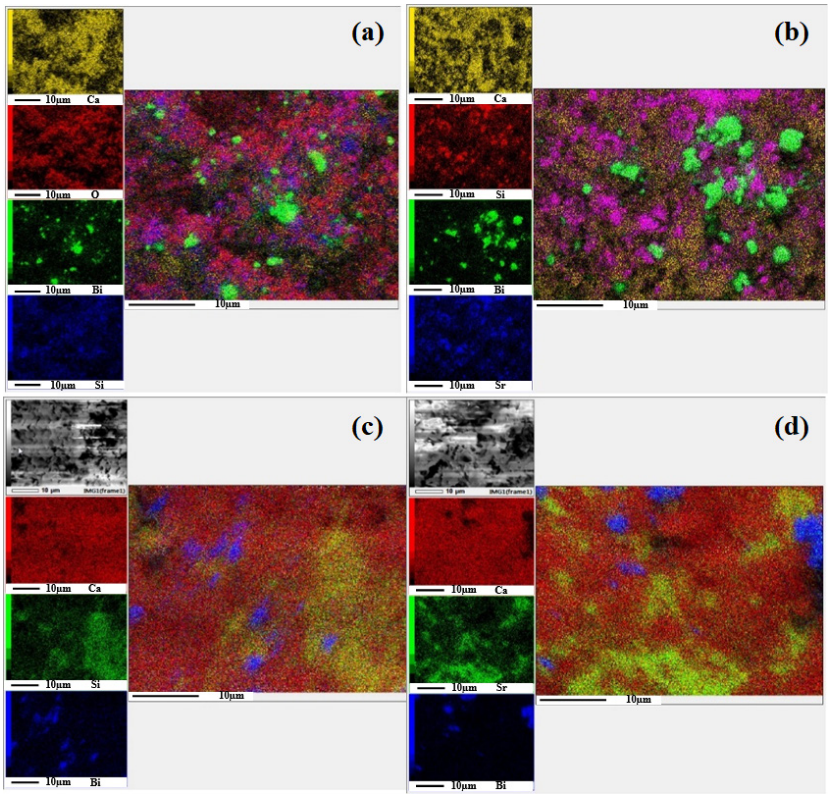

Fig. 8 Elemental mapping of un-hydrated materials: (a) MTAS0; (b) MTAS5 and after 7 days of hydration; (c) MTAS0; (d) MTAS5

The elemental mapping results in Fig. 8 demonstrate that calcium (yellow) is more concentrated in the MTA sample without SrO prior to hydration. In contrast, strontium (blue) is evenly distributed throughout the SrO-containing MTA, indicating effective incorporation of SrO into the matrix (Fig. 8 (b)). Bismuth oxide (green), which is introduced physically after calcination, displays a heterogeneous distribution, appearing in localized clusters rather than uniformly dispersed across the samples (Fig. 8 (a) and (b)). The unmodified MTA and MTAS5 samples also exhibit rough, irregular particle morphologies before hydration, reflecting their initial granular structure.

After 7 days of hydration, strontium (Fig. 8 (d)) remains homogeneously distributed within the matrix, although its surface intensity diminishes due to incorporation into aggregated hydration products. The relatively low SrO content (5 wt%) also reduces visibility in the elemental maps post-hydration. Bismuth oxide continues to exhibit uneven dispersion, attributable to its hydrophobic nature, which restricts interaction with water and can hinder hydration, leading to bubble formation that negatively impacts compressive strength [22]. Hydration produces substantial structural and compositional changes: the cement matrix becomes denser and smoother, with strontium uniformly integrated to reinforce mechanical performance, maintain an alkaline environment, and promote C–S–H formation.

4 Conclusion

The incorporation of 10% SrO into hydrated MTA results in the highest compressive strength, while the optimum HA content was identified at 3 wt%. Further addition of HA tends to reduce compressive strength, due to its bioactive characteristic, which does not enhance mechanical performance. All tested materials exhibit alkaline properties with pH values exceeding 7 after 28 days of hydration, demonstrating the stability of cement formation. Although initial mass loss following immersion is relatively high, MTA containing 5% SrO and 9% HA demonstrate improved stability with mass loss below 3%. Stable calcium ion release after 28 days is observed for MTA modified with 5% SrO and 6% HA, indicating successful hydrated product formation. Structural analysis reveals that adding 5% SrO and 6% HA enhances the intensity of C–S–H peaks. In comparison, the inclusion of 6% HA reduces Si–O–Si bonding intensity, suggesting changes in the hydration process. Overall, hydration induces aggregation, decreases porosity, and alters the microstructure of the cement matrix. Future investigations should address the antibacterial efficacy, biocompatibility, and other biological properties further to validate the clinical potential of these modified MTA formulations.

Acknowledgement

The project was partly funded by the Research Organization for Nanotechnology and Materials–National Research and Innovation Agency (BRIN) research grant 2025, Rumah Program Research Organization For Health 2025, and The Research and Innovation for Advanced Indonesia (RIIM) Competition 2025 Batch 7 from LPDP R1 with contract number B-3864/II/.7.5/KS.00/4/2025.

References

[1] Yuliatun, L., Kunarti, E. S., Widjijono, W., Nuryono, N. "Enhancing Compressive Strength and Dentin Interaction of Mineral Trioxide Aggregate by Adding SrO and Hydroxyapatite", Indonesian Journal of Chemistry, 22(6), pp. 1651–1662, 2022. https://doi.org/10.22146/ijc.76231

[2] Barbosa, A. M., dos Santos, K. W., Gonçalves, I. S., Leite, P. M. S. C. M., Martorano, A. S., Grisote, G., Castro-Raucci, L. M. S., de Oliveira, P. T., Raniero, L., Oliveira, I. R. "Calcium Aluminate Cement Blends Containing Bioactive Glass and Strontium for Biomaterial Applications", Materials Research, 24(6), e20210223, 2021. https://doi.org/10.1590/1980-5373-MR-2021-0223

[3] Elabbasy, M. T., Abd El-Kader, M. F. H., Ismail, A. M., Menazea, A. A. "Regulating the function of bismuth (III) oxide nanoparticles scattered in Chitosan/Poly (Vinyl Pyrrolidone) by laser ablation on electrical conductivity characterization and antimicrobial activity", Journal of Materials Research and Technology, 10, pp. 1348–1354, 2021. https://doi.org/10.1016/j.jmrt.2020.12.109

[4] ISO "ISO 6876:2001 Dental root canal sealing materials", International Organization for Standardization, Geneva, Switzerland, 2001.

[5] ANSI/ADA "ANSI/ADA 57-2021 Endodontic Sealing Materials", American National Standards Institute, American Dental Association, Chicago, IL, USA, 2021.

[6] Abdalla, M. M., Sayed, O., Lung, C. Y. K., Rajasekar, V., Yiu, C. K. Y. "Applications of Bioactive Strontium Compounds in Dentistry", Journal of Functional Biomaterials, 15(8), 216, 2024. https://doi.org/10.3390/jfb15080216

[7] You, J., Zhang, Y., Zhou, Y. "Strontium Functionalized in Biomaterials for Bone Tissue Engineering: A Prominent Role in Osteoimmunomodulation", Frontiers in Bioengineering and Biotechnology, 10, 928799, 2022. https://doi.org/10.3389/fbioe.2022.928799

[8] Mondal, S., Park, S., Choi, J., Vu, T. T. V., Doan, V. H. M., Vo, T. T., Lee, B., Oh, J. "Hydroxyapatite: A journey from biomaterials to advanced functional materials", Advances in Colloid and Interface Science, 321, 103013, 2023. https://doi.org/10.1016/j.cis.2023.103013

[9] Rheima, A. M., Abdul-Rasool, A. A., Al-Sharify, Z. T., Zaidan, H. K., Athair, D. M., Mohammed, S. H., Kianfar, E. "Nano bioceramics: Properties, applications, hydroxyapatite, nanohydroxyapatite and drug delivery", Case Studies in Chemical and Environmental Engineering, 10, 100869, 2024. https://doi.org/10.1016/j.cscee.2024.100869

[10] Twinprai, N., Sutthi, R., Ngaonee, P., Chaikool, P., Sookto, T., Twinprai, P., Mutoh, Y., Chindaprasirt, P., Laonapakul, T. "Effects of hydroxyapatite content on cytotoxicity, bioactivity and strength of metakaolin/hydroxyapatite composites", Arabian Journal of Chemistry, 17(9), 105878, 2024. https://doi.org/10.1016/j.arabjc.2024.105878

[11] Adamski, R., Siuta, D. "Mechanical, Structural, and Biological Properties of Chitosan/Hydroxyapatite/Silica Composites for Bone Tissue Engineering", Molecules, 26(7), 1976, 2021. https://doi.org/10.3390/molecules26071976

[12] Lunawat, K., Kavitha, S., Rajkumar, G., Dhivya, V., Ravi Kumar, N., Mahalaxmi, S., Shaik, F. A. "Influence of strontium containing fluorophosphate glass onto structural and mechanical behavior of MTA network", Journal of the Mechanical Behavior of Biomedical Materials, 140, 105750, 2023. https://doi.org/10.1016/j.jmbbm.2023.105750

[13] Mariyam, M., Sunarintyas, S., Yuliatun, L., Irnawati, D., Hatmanto, A. D., Nuryono, N. "Physicochemical and antibacterial properties of ZnO/chitosan-modified mineral trioxide aggregate composites", Case Studies in Chemical and Environmental Engineering, 9, 100749, 2024. https://doi.org/10.1016/j.cscee.2024.100749

[14] ISO "ISO 9917-1:2025 Dentistry — Water-based cements — Part 1: Acid-base cements", International Organization for Standardization, Geneva, Switzerland, 2025.

[15] Prakash, V., Darsini, H., Karthick, A., Venkatesh, A. "Mineral Trioxide Aggregate (MTA) – an overview", European Journal of Molecular & Clinical Medicine, 7(3), pp. 2115–2120, 2020. [online] Available at: https://www.ejmcm.com/archives/volume-7/issue-3/6727 [Accessed: 16 May 2025]

[16] Kahlenberg, V., Prosser, L., Salzmann, M. F., Hejny, C. "On the incorporation of strontium into the crystal structure of bredigite: structural effects and phase transition", Mineralogy and Petrology, 116(2), pp. 151–167, 2022. https://doi.org/10.1007/s00710-021-00771-x

[17] Lin, K.-L., Lin, W.-T., Chen, S.-C., Sprince, A. "Study on the cementation and engineering properties of ternary eco-binder mortar containing pulverized coal fly ash mixed with circulating fluidized bed co-fired fly ash", Journal of CO_2 Utilization, 83, 102787, 2024. https://doi.org/10.1016/j.jcou.2024.102787

[18] Vaiani, L., Boccaccio, A., Uva, A. E., Palumbo, G., Piccininni, G., Guglielmi, P., Cantore, S., Santacroce, L., Charitos, I. A., Ballini, A. "Ceramic Materials for Biomedical Applications: An Overview on Properties and Fabrication Processes", Journal of Functional Biomaterials, 14(3), 146, 2023. https://doi.org/10.3390/jfb14030146

[19] Brochu, B. M., Sturm, S. R., Kawase De Queiroz Goncalves, J. A., Mirsky, N. A., Sandino, A. I., …, Coelho, P. G. "Advances in Bioceramics for Bone Regeneration: A Narrative Review", Biomimetics, 9(11), 690, 2024. https://doi.org/10.3390/biomimetics9110690

[20] TanomaruFilho, M., Morales, V., da Silva, G. F., Bosso, R., Reis, J. M. S. N., Duarte, M. A. H., GuerreiroTanomaru, J. M. "Compressive Strength and Setting Time of MTA and Portland Cement Associated with Different Radiopacifying Agents", International Scholarly Research Notices, 2012(1), 898051, 2012. https://doi.org/10.5402/2012/898051

[21] Kim, J., Kim, H.J., Chang, S. W., Oh, S., Kim, S.-Y., Choi, K.-K., Kim, D.-S., Jang, J.-H. "Effect of bioactive glass addition on the physical properties of mineral trioxide aggregate", Biomaterials Research, 25(1), 39, 2021. https://doi.org/10.1186/s40824-021-00238-2

[22] Yuliatun, L., Lubis, M. A. R., Kusala, M. K. J., Destiarti, L., Betriani, R., Budiarta, J., Mariyam, M. "Radiographic, mechanical, and chemical properties of mineral trioxide aggregate from nanosilica and clam shell calcium carbonate", Polyhedron, 278, 117590 2025. https://doi.org/10.1016/j.poly.2025.117590

[23] Yuliatun, L., Nuswantoro, N. F., Lubis, M. A. R., Betriani, R., Budiarta, J., Destiarti, L., Ariyanti, D., Sari, E. P., Mariyam, M. "Effect of calcination temperature on the preparation of mineral trioxide aggregate from nano silica and clam shells calcium carbonate for endodontic applications", Journal of the Australian Ceramic Society, 2025. https://doi.org/10.1007/s41779-025-01244-6

[24] Loh, P.-Y., Shafigh, P., Ibrahim, Z. "The pH measurement of cement-based materials: Effect of leaching time, leaching technique and water-to-solid ratio", Construction and Building Materials, 411, 134525, 2024. https://doi.org/10.1016/j.conbuildmat.2023.134525

[25] Zhang, G., Wu, C., Hou, D., Yang, J., Sun, D., Zhang, X. "Effect of environmental pH values on phase composition and microstructure of Portland cement paste under sulfate attack", Composites Part B: Engineering, 216, 108862, 2021. https://doi.org/10.1016/j.compositesb.2021.108862

[26] Montesi, M., Panseri, S., Dapporto, M., Tampieri, A., Sprio, S. "Sr-substituted bone cements direct mesenchymal stem cells, osteoblasts and osteoclasts fate", PLoS ONE, 12(2), e0172100, 2017. https://doi.org/10.1371/journal.pone.0172100

[27] Bortoluzzi, E. A., Broon, N. J., Bramante, C. M., Garcia, R. B., de Moraes, I. G., Bernardineli, N. "Sealing Ability of MTA and Radiopaque Portland Cement With or Without Calcium Chloride for Root-End Filling", Journal of Endodontics, 32(9), pp. 897–900, 2006. https://doi.org/10.1016/j.joen.2006.04.006

[28] Shashank, S., Jaiswal, S., Nikhil, V., Gupta, S., Mishra, P., Raj, S. "Comparative pH and calcium ion release in newer calcium silicate-based root canal sealers", Endodontology, 31(1), pp. 29–33, 2019. https://doi.org/10.4103/endo.endo_53_18

[29] Ochoa-Rodríguez, V. M., Coaguila-Llerena, H., Fernandes, L., B. Solcia, A. B., Guerreiro-Tanomaru, J. M., Tanomaru-Filho, M., Faria, G. "Evaluation of Solubility, and Volumetric and Morphological Alterations of Bioceramic Filling Material for Primary Teeth: A New Methodological Approach", International Journal of Dentistry, 2024(1), 5945033, 2024. https://doi.org/10.1155/2024/5945033

[30] Matović, I., Vučcetić, J. "Stability and solubility test of endodontic materials", Stomatološki Glasnik Srbije, 69(4), pp. 169–174, 2022. https://doi.org/10.2298/sgs2204169m

[31] Kaysım, M. G., Kumlay, A. M., Haliloglu, K., Türkoğlu, A., Piekutowska, M., Nadaroğlu, H., Alayli, A., Niedbała, G. "Physiological and Antioxidative Effects of Strontium Oxide Nanoparticles on Wheat", Agronomy, 14(4), 770, 2024. https://doi.org/10.3390/agronomy14040770

[32] Harrison, C. J., Hatton, P. V., Gentile, P., Miller, C. A. "Nanoscale Strontium-Substituted Hydroxyapatite Pastes and Gels for Bone Tissue Regeneration", Nanomaterials, 11(6), 1611, 2021. https://doi.org/10.3390/nano11061611

[33] ISO "ISO 6876:2012 Dentistry — Root canal sealing materials", International Organization for Standardization, Geneva, Switzerland, 2012.

[34] Sprio, S., Dapporto, M., Preti, L., Mazzoni, E., Iaquinta, M. R., Martini, F., Tognon, M., Pugno, N. M., Restivo, E., Visai, L., Tampieri, A. "Enhancement of the Biological and Mechanical Performances of Sintered Hydroxyapatite by Multiple Ions Doping", Frontiers in Materials, 7, 224, 2020. https://doi.org/10.3389/fmats.2020.00224

[35] Mariyam, M., Sunarintyas, S., Nuryono, N. "Improving mechanical, biological, and adhesive properties of synthesized mineral trioxide aggregate by adding chitosan", Inorganic Chemistry Communications, 149, 110446, 2023. https://doi.org/10.1016/j.inoche.2023.110446

[36] Rathinam, E., Govindarajan, S., Rajasekharan, S., Declercq, H., Elewaut, D., De Coster, P., Martens, L., Leybaert, L. "The calcium dynamics of human dental pulp stem cells stimulated with tricalcium silicate-based cements determine their differentiation and mineralization outcome", Scientific Reports, 11(1), 645, 2021. https://doi.org/10.1038/s41598-020-80096-5

[37] Abu Zeid, S. T., Alamoudi, N. M., Khafagi, M. G., Abou Neel, E. A. "Chemistry and Bioactivity of NeoMTA Plus™ versus MTA Angelus® Root Repair Materials", Journal of Spectroscopy, 2017(1), 8736428, 2017. https://doi.org/10.1155/2017/8736428

[38] Pelepenko, L. E., Marciano, M. A., Francati, T. M., Bombarda, G., Bessa Marconato Antunes, T., …, Camilleri, J. "Can strontium replace calcium in bioactive materials for dental applications ?", Journal of Biomedical Materials Research Part A, 110(12), pp. 1892–1911, 2022. https://doi.org/10.1002/jbm.a.37421

[39] Li, Q., Coleman, N. J. "The hydration chemistry of ProRoot MTA", Dental Materials Journal, 34(4), pp. 458–465, 2015. https://doi.org/10.4012/dmj.2014-309

[40] Cervino, G., Laino, L., D'Amico, C., Russo, D., Nucci, L., …, Fiorillo, L. "Mineral Trioxide Aggregate Applications in Endodontics: A Review", European Journal of Dentistry, 14(4), pp. 683–691, 2020. https://doi.org/10.1055/s-0040-1713073

[41] Abu Zeid, S. T., Edrees, H. Y. "Hydration Characterization of Two Generations of MTA-Based Root Canal Sealers", Applied Sciences, 12(7), 3517, 2022. https://doi.org/10.3390/app12073517

[42] Mahmoud, O., Al-Afifi, N. A., Salihu Farook, M., Ibrahim, M. A., Al Shehadat, S., Alsaegh, M. A. "Morphological and Chemical Analysis of Different Types of Calcium Silicate-Based Cements", International Journal of Dentistry, 2022(1), 6480047, 2022. https://doi.org/10.1155/2022/6480047

[43] Radeva, E., Uzunov, T. "Comparative SEM study of the marginal adaptation of MTA and Biodentine after apical resection (in vitro study)", Folia Medica, 65(2), pp. 269–276, 2023. https://doi.org/10.3897/folmed.65.e74030